Peculiarity of Radiation Distribution in Multi-Impurity seeded H-mode Plasmas on JET with ITER-like Wall

A. Huber[1], M. Wischmeier[2], M. Bernert[2], S. Wiesen[1], S. Glöggler[2], S. Aleiferis[3], S. Brezinsek[1], G. Calabro[4], P. Carvalho[5], V. Huber[6], G. Sergienko[1], E. R. Solano[7], C. Giroud[8], M. Groth[9], S. Jachmich[10], Ch. Linsmeier[1], G.F. Matthews[8], A.G. Meigs[8], Ph. Mertens[1], M. Sertoli[2], S. Silburn[8], G. Telesca[11] and JET Contributors[#]

[1]Forschungszentrum Jülich GmbH, Institut für Energie- und Klimaforschung – Plasmaphysik, Partner of the Trilateral Euregio Cluster (TEC), 52425 Jülich, Germany
[2]Max-Planck-Institut für Plasmaphysik, Boltzmannstraße 2, D-85748 Garching, Germany
[3]NCSR 'Demokritos', 153 10, Agia Paraskevi Attikis, Greece
[4]Department of Economics, Engineering, Society and Business Organization (DEIm), University of Tuscia, Largo dell'Università snc, 01100 Viterbo, Italy
[5]Instituto de Plasmas e Fusão Nuclear, Instituto Superior Técnico, Universidade de Lisboa, Portugal,
[6]Forschungszentrum Jülich GmbH, Supercomputing Centre, 52425 Jülich, Germany
[7]Laboratorio Nacional de Fusión, CIEMAT, Madrid, Spain
[8]CCFE, Culham Science Centre, Abingdon, OX14 3DB, UK
[9]Aalto University, Association EURATOM-Tekes, P.O.Box 4100, 02015 Espoo, Finland
[10]Laboratory for Plasma Physics, ERM/KMS, B-1000 Brussels, Belgium
[11]Institute of Plasma Physics and Laser Microfusion, Warsaw, Poland

E-mail: A.Huber@fz-juelich.de

Keywords: power exhaust, radiation, impurities in plasmas, divertors, detachment, tokamaks
PACS numbers: 52.55.Rk, 52.25.Vy, 52.40.Hf, 52.55.Fa

Abstract

On JET with fully metallic first wall, highly radiative conditions with N_2, Ne and Ar as well as their mixture as radiators are approached in high density H-mode plasmas. The confinement increases from $H_{98(y,2)}$=0.6 in unseeded pulses with γ_{rad}~30% to a value of $H_{98(y,2)}$=0.75 at γ_{rad}~50% with N_2 injection. A degradation of the pedestal profile is compensated by steeper core n_e and T_e profiles. Further increase of γ_{rad} with increase of the N_2 seeding rate leads to a moderate confinement degradation which can be avoided by applying of combined impurity seeding. The enhancement of the plasma performance for the radiation fractions beyond 55% with the maximum value of $H_{98(y,2)}$=0.78 is reached with combined N_2+Ne and N_2+Ar impurity injections. The observed intense, strongly localized radiation at the X-point inside the confined plasma in the scenarios with the highest radiated power fraction is interlinked to complete divertor detachment. In the JET-ILW, the X-point radiation is stable, reproducible and reversible.

1. Introduction

The development of high radiation plasma scenarios with impurity seeding is necessary for the safe operation of fusion devices with a burning plasma such as ITER and DEMO where perpendicular divertor target loads should be kept below 5−10MWm^{-2} [1,2] to avoid divertor damage. At the same time, the electron temperature at the target needs to be low enough to

[#] See the author list of "Overview of the JET preparation for Deuterium-Tritium Operation" by E. Joffrin et al. to be published in Nuclear Fusion Special issue: overview and summary reports from the 27th Fusion Energy Conference (Ahmedabad, India, 22-27 October 2018) limit the target plate erosion to acceptable values. However, radiative power losses within the confined plasma can affect the plasma confinement and fuel dilution as well as the discharge stability. Therefore, it is very important to understand underlying physical processes in highly radiative discharges to provide the recipe for controlled seeding with a sufficient reduction of the power flux and target temperature while minimizing the impact on the confined plasma.

Consequently, the selection of an extrinsic impurity for fusion devices is based on its radiative characteristics in the main plasma and in the divertor region as well as on its impact on the plasma confinement with a high divertor radiation. Also the interaction of the seeded impurities with the PFCs and its consequences for the tritium processing plant should be taken into account. In the present tokamak experiments nitrogen is favoured as divertor radiator since it is generally observed to be more efficiently compressed than Ne, providing more localized divertor radiation [3,4,5]. However, nitrogen is chemically active and can lead to the formation of ammonia which, in the case of deuterium-tritium operation in ITER, will produce tritiated ammonia (NT_3) [6]. The amount of NT_3 produced may be significant and could have an impact on the exhaust treatment, which will affect the design of the ITER tritium plant. In contrast to the experimental observations, simulations for ITER at high performance [7] indicate that compression for N_2 and Ne will be similar. In addition, Ne is not chemically reactive, which makes it an attractive candidate as a divertor radiator in ITER. In addition to N_2 and Ne, Argon is considered also as further candidate for simultaneous enhancement of core and divertor radiation, when some increased main chamber radiation is desired as well. It is assumed that sufficient divertor compression for Ar can be obtained.

Impurities, such as nitrogen (N_2), neon (Ne) and argon (Ar), are widely used in radiative divertor experiments on several tokamaks [8,9,10]. On the other hand, interpretation studies on mixed seed discharges in tokamaks have not been performed very often [11,12]. Therefore, more investigations on mixed seeding experiments need to be carried out to develop scenarios with sufficient energy confinement simultaneously with a high radiation level.

2. Impurity seeding in high-density H-mode plasmas

2.1 N_2 seeding in high density H-mode plasmas

After JET first wall has been upgraded with a new ITER-like wall (ILW) [13], the level of carbon is reduced at least by a factor of 10 [14] leading to a strong reduction of the divertor radiation in the fully metallic machine.

Nitrogen turns out to be a suitable replacement for carbon as a divertor radiator thanks to its maximum radiative efficiency at low temperatures, T_e~10-20eV [15]. Dedicated H-mode nitrogen seeding experiments have been performed at JET with ITER-like wall to investigate the impact of impurity seeding on the energy confinement as well as its dependence on the balance between main chamber and divertor radiation. High density Type I H-mode plasmas at B_T=2.7T, I_p=2.5MA (q_{95}=3.3) at Greenwald density fraction f_{GW} (=$\langle n_e\rangle/n_{e,GW}$) up to 85% in low-triangularity magnetic equilibria (δ=0.22) with both strike points on the lower vertical targets have been examined. Thereby, the Greenwald density limit $n_{e,GW}$ [10^{20} m^{-3}]=I_p [MA]/(πa^2) and a is the plasma minor radius in m [16]. Respective scans have been performed over a deuterium fuelling range of 2×10^{22}el/s÷6.5×10^{22} el/s and an impurity seeding range of 2×10^{22}el/s÷1.3×10^{23} el/s with an auxiliary heating power of 18MW. Time traces of a typical N_2 seeded discharges at n/n_{GW}~0.85 are shown in Fig. 1a. The BeII fast emission signal (λ=527nm) in the outer divertor represents the ELM behaviour. In contrast to an unseeded plasma (not shown in the figure), the N_2 seeding into the private flux of the outer divertor leg with $\Gamma_{N2}\approx13.4\times10^{22}$el/s

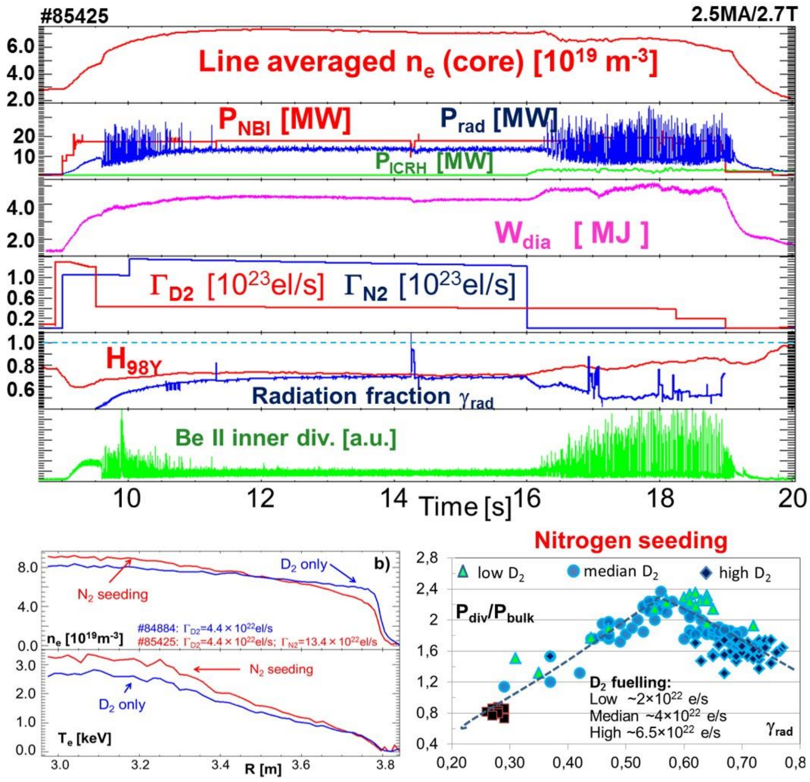

Fig.1 a) Time traces of central line averaged n_e, NBI and ICRH heating power as well as total radiated power, plasma stored energy, D_2-fuelling and N_2-seeding waveforms, γ_{rad} and $H_{98(y,2)}$-factor, BeII fast emission signal in the inner divertor of a N_2-seeded high-density H-mode plasma on JET-ILW b) comparison of n_e and T_e profiles for nitrogen c) radiation distribution in the main chamber versus divertor region.

demonstrates directly after the L-H transition small energy ELMs with a quick transition at 10.8s from a type I ELMy to a stable and steady state ELM-free H-mode phase with cold pedestal ($T_e^{ped}\approx$300eV) and some recovery of the energy confinement (Fig.1a). During this ELM free H-mode, the so-called M-mode [17] with plasma performance between L-mode and H-mode (medium confinement), the radiation fraction reaches the value of γ_{rad} ~75%. This mode can typically be observed during the operation with the input power close to the L-H power threshold or just right after an L-H transition. During the M-mode phase the characteristic oscillation can be seen in the fast divertor D_α emissions as well as in the signals of a poloidal Mirnov coil.

In the unseeded plasma, the global confinement was significantly degraded at increasing fuelling levels to reach a high density close to Greenwald limit [16]. In comparison with the unseeded pulse, Z_{eff} increases during the seeding with N_2 by ≈50% (increase of ΔZ_{eff}=0.6). The radiation fraction in this pulse reaches its peak-value of about 75%. Considerable energy confinement recovery is observed with N_2 seeding. It increases from a confinement factor of $H_{98(y,2)}$=0.65 in the pulse with D_2 fuelling only to a factor of $H_{98(y,2)}$=0.75. Figure 1b shows profiles of the temperature T_e and electron density n_e measured by the High Resolution Thomson Scattering system [18] in unseeded as well as seeded plasmas. In contrast to the unseeded plasma, the electron density n_e in the nitrogen seeded plasmas decreases in the edge region and increases in the plasma core correspondingly, demonstrating a more significantly peaked behaviour (see Fig.1b). This steepening is explained using ASTRA-TGLF simulations by a stabilizing effect on the ITG modes through dilution of the main ion density [21]. On the other hand, T_e rises across the entire profile with N_2 seeding. Consequently, the impurity seeding strongly affects the particle transport and confinement, thus possibly increasing the energy stored in the plasma. In contrast to these experiments, the N_2 seeding in JET-ILW in high triangularity geometry demonstrates an enhanced energy confinement due to an improved pedestal [9]. Also the plasma performance improvement with nitrogen is observed on ASDEX Upgrade where the improvement is clearly related to the improved pedestal performance [19].

Fig.1c shows the radiation distribution in the main chamber versus divertor region in the plasmas with injected N_2. In this contribution, the divertor radiation P_{div} is defined as the radiation emitted below $Z \leq -1.0$m, and $P_{rad}^{bulk}=P_{rad}^{tot}-P_{rad}^{div.}$. For the characterisation of the radiation distribution, we are using here the ratio of radiation fractions in divertor and main chamber ($P_{rad}^{div}/P_{rad}^{bulk}$). This evaluated ratio, as well as γ_{rad}^{div}, does not show a clear dependence on D_2-fueling in N_2-seeded, type-I ELMy H-mode pulses. The fraction of the divertor radiation increases initially with increase of the radiation fraction and reach the maximal value at γ_{rad}~55-60%. Additional increase of γ_{rad} leads to a reduction of the $P_{rad}^{div}/P_{rad}^{bulk}$ indicating some level of saturation in the divertor radiation.

2.2 Ne and Ar seeding in high density H-mode plasmas

In addition to N_2 seeded scenarios, high radiation scenarios with Ne and Ar seeding were tested at JET. Neon is a promising candidate as an edge radiating impurity for future reactor scenarios radiating dominantly at temperatures of about 50eV [15].

As is discussed in [3], Ar and Ne seeding increased the fraction of the total radiation up to a level of 63% which is below that of the highest N_2 cases of 75% . The radiation distribution inclined slightly more biased towards the plasma core with contribution of about half of radiation fraction ($\gamma_{rad}^{div}\approx0.5$) in the divertor region, as one might expect from the temperature dependence of the radiative cooling efficiency function [15]. In contrast to N_2 injection which causes a considerable improvement of the energy confinement, the Ar seeding causes only a moderate one. Ne and Ar also radiate in the pedestal and main plasma (respectively) reducing the power entering the edge region and as a result reducing the pedestal confinement [3, 5]. It was observed, that seeding with Ar leads to an H-L transition at radiation fraction γ_{rad} of ~60% [3].

As demonstrated in details in [3], the neon seeded discharges showed beyond γ_{rad} ~50% an ELM-free phase (or M-mode) with a sequence of H-L-H transitions. During the transient L-mode periods of these transitions, the γ_{rad} increases up to 95%, whereas the electron density is decreasing in the edge and in the core. The radiation profiles show completely different behaviours during the transition cycles as shown in [3]: during the L-mode period, the radiation pattern is located around the X-point with strong contributions in the outer and inner SOL; during the H-mode phase (or M-mode), the radiation is peaked in the region above the X-point inside the separatrix. During the ELM-free H-mode (or M-mode) phases with Ne seeding, an improvement of the confinement factor up to $H_{98(y,2)}\approx0.75$ at γ_{rad}~50% is observed. At the same time, Z_{eff} is increasing for the duration of the seeding by ≈80% (increase of $\Delta Z_{eff}=0.9$) in comparison with unseeded plasma.

2.3 Combined N_2 and Ne seeding in H-mode plasmas

A detailed study of the synergistic effects of combined impurity injections is required to predict the applicability of such scenarios to future devices. Fig.2 shows the temporal evolution of the plasma parameters with a combination gas seeding of N_2 and Ne. The discharge (I_P/B_T=2.5MA/2.7T) is performed in vertical target divertor geometry at the low triangularity configuration ($\delta_{av}\approx0.25$). NBI and ICRH heating powers were 18 MW and 4.0MW respectively to maintain the plasma stored energy (W_{dia}) of 5.2 MJ. The nitrogen and neon are injected at the horizontal tiles into the private flux region (PFR). The N_2 injection is started during the ramp-up phase in order to avoid the high heat loads on the divertor and to prevent W sputtering and its accumulation during this phase. The N_2 injection provokes the increase of the radiation fraction which reaches a quasi-stationary level of about 60% prior to the Ne injection phase (Z_{eff}=2.0). Before the Ne seeding, the divertor is in a fully detached state and the normalized confinement following the ITER physics base scaling is around $H_{98(y,2)}$=0.71 at about 85% of the Greenwald density. No significant heat flux is measured at the divertor targets. From t=11s, the small Ne gas puff is injected into the divertor (injection rate of 1.4×10^{21}el/s). By adding a small amount of seeded Ne (seeded fraction of $\Gamma_{Ne}/\Gamma_{N2}\approx1\%$) to the N_2 puff, particle confinement and transport could be significantly improved. T_e rises in the plasma core without pedestal alteration. The core electron temperature was measured by the electron cyclotron emission (ECE) diagnostic [20]. Z_{eff} increases during the combined seedings and reaches the value of 2.35 at t=53.1s. Additionally, fig.2 shows an increase of the plasma stored energy during the combined seeding phase. As a result, using a combination of the N_2 and Ne gas seeding (51.4-54s), good confinement ($H_{98(y,2)}$=0.78) with high radiation fraction (γ_{rad}=0.7) was reached in high density Type-I ELMy H-mode.

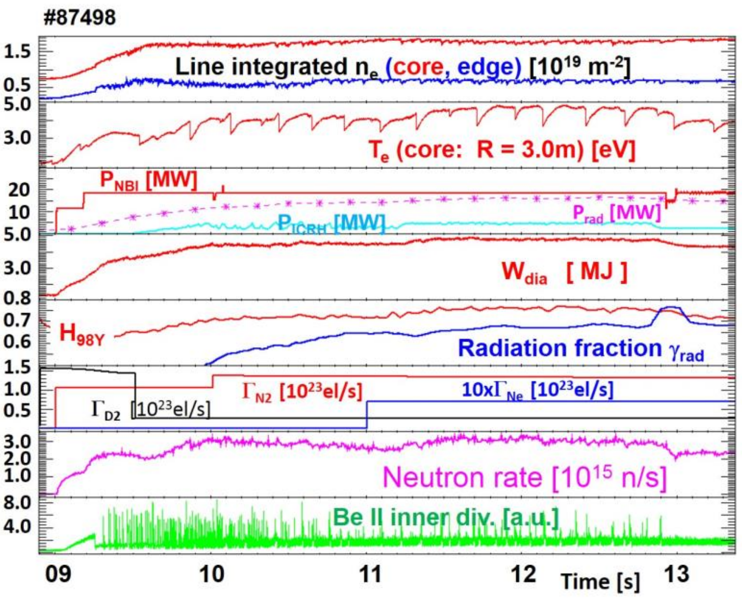

Fig.2: Time traces of combined N_2+Ne seeded ELMy H-mode discharge in JET-ILW (#87498). From top: line-integrated core and edge electron density measured by interferometer, T_e at R=3.0m measured by the ECE diagnostic, NBI and ICRH heating power as well as total radiated power , diamagnetic stored energy, $H_{98(y,2)}$ confinement factor and γ_{rad}, D2-fuelling and N_2- and Ne-seeding waveforms, neutron rate, BeII fast emission signal in the outer divertor.

Also a slight increase of the neutron rate is observed during the phase with combined N_2 and Ne seeding. In the plasmas studied here, the neutrons are primarily created by the interaction of the NBI beams with the thermal deuterons. This result is consistent with the observations reported in [21] where the neutron rate increases with increased neon puffing in the experiments under experimental conditions similar to those reported here.

Fig.3 shows the radiation distributions and the vertical Z-averaged radiation distributions for H-mode plasmas with N_2 seeding only as well as for combined N_2 and Ne seeding. The tomographically reconstructed radiation distribution shows intense radiation in the vicinity of the X-point for N_2 seeded plasmas as well as for plasmas with combined impurities injection. This observation is consistent with the statement given in [22] where it is reported that for conductive parallel heat flow, the radiation in the SOL will peak in the region of the largest parallel temperature gradients. The largest parallel temperature gradients are expected close to the divertor and around the X-point. The radiation distribution extends from the X-point peak its ‘wing-like’ pattern upwards along the separatrix towards the inside and outside mid-plane positions. As can be seen, it decreases strongly as one moves away from the divertor. These findings are approximately consistent with the expected parallel temperature gradient along the SOL.

Adding a small amount of seeded Ne (seeded fraction of $\Gamma_{Ne}/\Gamma_{N2}\approx 1\%$) increased strongly the radiation around X-point (Fig.3) without altering the radiation in the main chamber as shown in the vertical Z-averaged radiation distribution (fig.3a). The increased seeded fraction to $\Gamma_{Ne}/\Gamma_{N2}\approx 4\%$ at the middle seeding rate ($\Gamma_{N2}\approx 7.6\times 10^{22}$el/s) increased significantly the X-point radiation and only moderately the core radiation (fig.3b) without visible impact on the energy confinement.

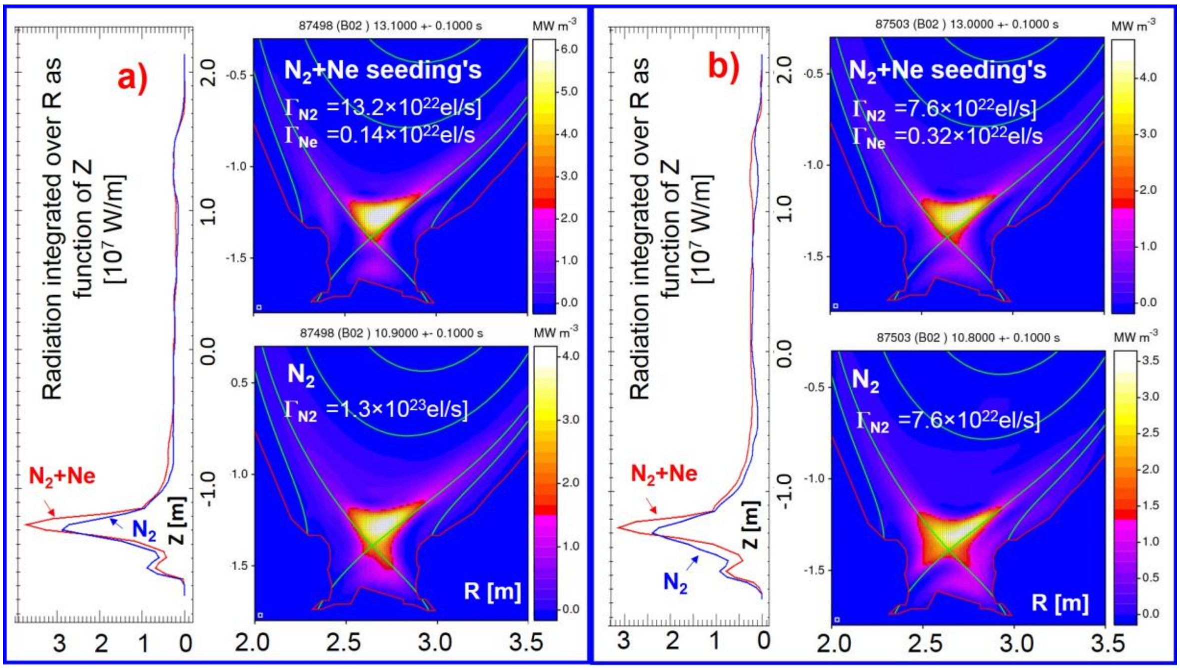

Fig.3 The vertical Z-averaged radiation distribution as well as tomographic reconstructions of the bolometric data for N_2 seeded as well as for the simultaneous N_2 and Ne injections. Figures a) and b) represent the cases with different impurity seeding rates as well as with different Γ_{Ne}/Γ_{N2} ratios. During the combined impurity seeding, Z_{eff} reaches the values of 2.3 (Fig.3b) and 2.35 (Fig.3a) (Fig.3b).

2.4 Combined N_2 and Ar seeding in H-mode plasmas

The radiation enhancement in the SOL region is more pronounced for the lower-Z atoms such as N_2 and Ne compared to Ar. The cooling efficiency of Ar peaks at $T_e\sim 20$ eV and ~200 eV compared with that of N and Ne ions, which has a peak at 20–50 eV [15]. It is worth to mention that the cooling efficiency of Ar is higher than that of the lighter species, such as Ne and N_2. Correspondingly, argon exhibits the highest radiative efficiency for the temperature range of the divertor. However, its high radiative losses in the core plasma do not permit high Ar concentrations unless a very high compression in the divertor can be obtained [10]. Combined gas seeding of N_2 and Ar gas seeding was investigated in high density H-mode discharges.

Fig.4 shows the radiation distributions and the vertical Z-averaged radiation distributions for H-mode plasmas with N_2 seeding only as well as for combined N_2 and Ar injection. The nitrogen and Ar are injected at constant seeding rates of $\Gamma_{N2}\approx1.04\times10^{23}$el/s ($1.1 \times 10^{23}$ el/s in Fig.4b) and $\Gamma_{Ar}\approx0.41\times10^{22}$el/s ($8.2\times10^{22}$el/s in Fig.4b) which corresponds to the impurity seeded mixed fraction of $\Gamma_{Ar}/\Gamma_{N2}\approx4\%$ (74% in Fig.7b). For both cases, with N_2 only seeding

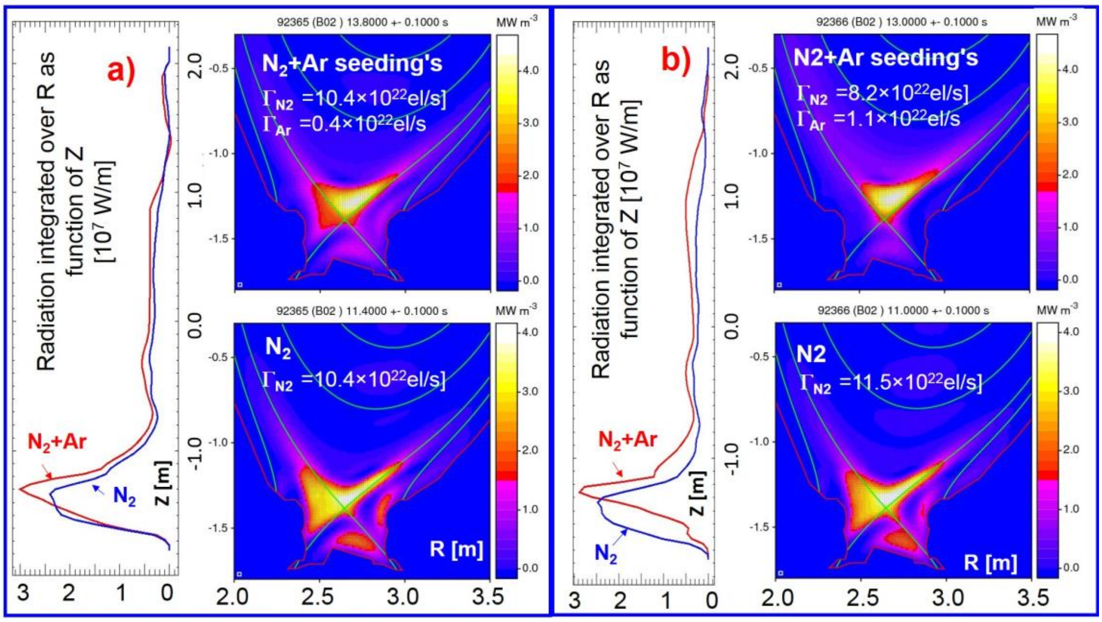

Fig.4 The vertical Z-averaged radiation distribution as well as tomographic reconstructions of the bolometric data for N_2 seeded and for the simultaneous N_2 and Ar injections. Figures a) and b) represent the cases with different impurity seeding rates as well as with different Γ_{Ar}/Γ_{N2} ratios.

($Z_{eff}\approx1.85$) as well as with combined N_2 and Ar injections ($Z_{eff}\approx2.15$ (Fig.4a) and $Z_{eff}\approx2.3$ (Fig.4b)), the dominant radiation originates from the confined region and is concentrated in a region close to the X-point. Nevertheless, in contrast to combined impurity puffing, the radiation in the inner divertor is clearly visible for the plasma with N_2 cooling alone. From the X-point peak, the radiation distribution with combined impurity injections extends much strongly the 'wings-like' pattern upwards along the separatrix towards the inside and outside mid-plane positions. A significant increase of the radiation in the main plasma can be clearly seen in the vertical Z-averaged radiation distributions (Fig.4a,b). These vertical distributions (Fig.4a,b) do not show any significant improvement in the peak divertor radiation.

On the other hand, the location of maximum radiation moves to the direction of the main chamber. These results are consistent with tomographic reconstructions of the radiation distributions: in the combined seeding scenario (N_2+Ar) radiation "spills over" into the region above the X-point inside of the separatrix.

3. Confinement in high-density highly radiative H-mode plasma scenarios

With regard to future fusion devices, the effect of various seed impurities on the plasma confinement needs to be investigated. Fig.5 shows the confinement factor $H_{98(y,2)}$, measured during the experiments with three seeded impurity species N_2, Ne and Ar, as a function of radiated power fraction. The plasma performance in the N_2 seeded plasmas was analysed over a deuterium fuelling range of 2×10^{22}el/s÷6.5×10^{22}el/s and an impurity seeding range of 2×10^{22} el/s÷1.3×10^{23}el/s. The confinement increases from $H_{98(y,2)}$=0.6 in unseeded pulses with γ_{rad}~30% to a value of $H_{98(y,2)}$=0.75 at γ_{rad}~50% with N_2 injection. As it is discussed in section 2.1, the N_2 seeding significantly affects the particle confinement and transport increasing the energy stored in the plasma: the degraded electron density pedestal is accompanied by an n_e increase in the plasma core as well as an increase of the electron temperature T_e in the core. Further increase of γ_{rad} with increase of the N_2 seeding rate leads to a moderate confinement degradation. Beyond γ_{rad}~55%, the energy confinement scaling factor remains almost constant at ≈0.7.

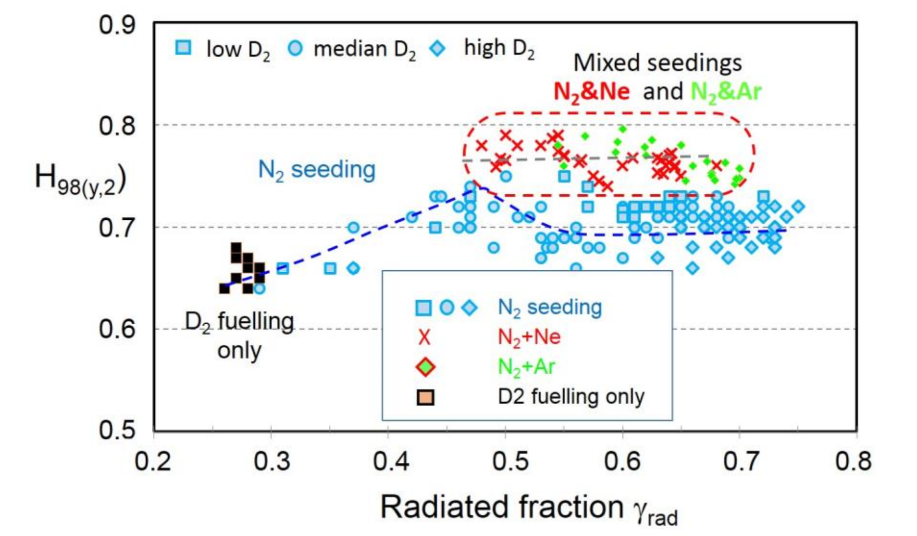

Fig.5 $H_{98(y,2)}$ as a function of radiated power fraction. Improved confinement for combined N_2+Ne as well as N_2+Ar radiators is approached in high density, highly radiative H-mode plasma scenarios.

The confinement improvement during the N_2 seeding in JET-ILW is in contrast to findings seen in JET-C with a carbon divertor, where a reduction of $H_{98(y,2)}$ was always observed during impurity seeding [23,24]. Comparison of the thermal energy confinement for the unseeded discharges as well as for three seeding scenario cases is shown in fig.5. This figure demonstrates the further enhancement of the plasma performance for the radiation fractions beyond 55%. The maximum value of $H_{98(y,2)}$=0.78, reached at combined N_2+Ne and N_2+Ar impurity injections, is lower than required for ITER. It should be noted, however, that the unseeded discharges have already a low confinement factor $H_{98(y.2)}$ of about 0.65. Therefore, the impurity seeded ELMy H-mode discharges allow operation at higher densities compared to unseeded reference discharges, with good confinement or at least without a strong degradation of the confinement, as illustrated in Fig.5.

Conclusion

To find the optimum proportion of multiple seeded impurity species (Ne, Ar, N_2) compatible with a high confinement, dedicated H-mode impurity seeding experiments with different mixtures of seeded impurities have been performed in JET-ILW. We investigated how different mixtures influence the radiation patterns, radiation distributions as well as the confinement in the divertor and in the plasma core. The nitrogen causes a considerable energy confinement recovery from a confinement factor of $H_{98(y,2)}\approx0.65$ in the discharge with D_2 fuelling only to a factor of $H_{98(y,2)}\approx0.75$ at $\gamma_{rad}\sim50\%$. Further increase of γ_{rad} with increase of the N_2 seeding rate leads, however, to a moderate confinement degradation. These losses of the plasma performance for the radiation fractions beyond 55% can be recovered by applying of combined N_2+Ne and N_2+Ar impurity injections. The confinement factor increased from 0.7 with N_2 seeding to the value of $H_{98(y,2)}=0.78$ (N_2+Ne or N_2+Ar seeding). By adding a small amount of seeded Ne (seeded fraction of $\Gamma_{Ne}/\Gamma_{N2}\approx1\%$) to the N_2 puff, particle confinement and transport is significantly affected. T_e rises in the plasma core without pedestal alteration. As a result, the energy stored in the plasma and the confinement factor are increased to $H_{98(y,2)}\approx0.78$. Also a good confinement of $H_{98(y,2)}\approx0.77$ at a seeded fraction of $\Gamma_{Ar}/\Gamma_{N2}\approx4\%$ has been demonstrated regardless of significant radiation from inside the separatrix.

The observed intense strongly localized radiation at the X-point inside the confined plasma is interlinked to a complete divertor detachment. It is demonstrated that the X-point radiation in the JET-ILW is stable, reproducible and reversible. The complete detachment of the divertor target is not associated with the occurrence of an H-mode density limit. These experiments with combined impurity seeding show that an increase of the radiation inside the separatrix has no impact on the energy confinement.

Based on the result of this contribution, a mix of impurities could be considered for ITER, a low-Z species for divertor radiation and a medium-Z species for radiation in the confined region to optimize the radiative power removal in the main plasma and the divertor region.

Acknowledgements

This work has been carried out within the framework of the EUROfusion Consortium and has received funding from the Euratom research and training programme 2014-2018 and 2019-2020 under grant agreement No 633053. The views and opinions expressed herein do not necessarily reflect those of the European Commission.

References

[1] Loarte A. et al 2007 Nucl. Fusion 47 S203–S263
[2] Raffray A R et al 2010 Fusion Eng. Des. 85 93–108
[3] Huber A et al Impact of Strong Impurity Seeding on the Radiation Losses in JET with ITER-like Wall, in: Proc. of the 41th EPS Conference on Controlled Fusion and Plasma Physics, Berlin, 2014), 2014 http://ocs.ciemat.es/EPS2014PAP/pdf/ P1.031.pdf , P1.031.
[4] Bernert M et al 2017 Nucl. Mater. Energy 12 111–118
[5] Wischmeier M et al 2015 J. Nucl. Mater. 463 22–29 ISSN 0022-3115
[6] Oberkofler M et al 2013 J. Nucl. Mater. 438 (2013) S258–S261
[7] Kukushkin A S et al 2011 Fusion Eng. Des. 86 2865, https://doi.org/10.1016/j. fusengdes.2011.06.009.
[8] Reinke M L et al 2011 J. Nucl. Mater. 415 S340–S344
[9] Giroud C et al 2013 Nucl.Fusion 53 113025
[10] Kallenbach A et al 2013 Plasma Phys. Control. Fusion 55 124041
[11] Asakura N et al 2009 Nucl. Fusion 49 115010 (2009).
[12] Kallenbach A et al 2012 Nucl. Fusion 52 122003
[13] Matthews G F et al 2011 Phys. Scr. T145 014001.
[14] Brezinsek S et al 2013 J. Nucl. Mater. 438 S303–S308
[15] Post D et al 1995 Phys. Plasmas 2 2328
[16] Greenwald M 2002 Plasma Phys. Control. Fusion 44 R27
[17] Solano E R et al 2017 Nuclear Fusion 57 022021
[18] Pasqualotto R et al 2004 Rev. Sci. Instrum. 75 3891
[19] Schweinzer J et al 2011 Nuclear Fusion 51 113003.
[20] de la Luna E et al 2004 Rev. Sci. Instrum. 75 3831
[21] S. Gloeggler to be published in Nucl. Fusion
[22] Pitcher C S and Stangeby P C 1997 Plasma Phys. Control. Fusion 39 779
[23] Maddison G. et al Nuclear Fusion 51 (2011) 042001.
[24] Giroud C et al 2012 Nucl. Fusion 52 063022.